Ultrastructural Changes in Skeletal Muscle of Infants with Mitochondrial Respiratory Chain Complex I Defects

Ji Young Mun[a]*
Min Kyo Jung[b]*
Se Hoon Kim[c]
Soyong Eom[d]
Sung Sik Han[b]
Young-Mock Lee[e]

[a]Department of Biomedical Laboratory
 Science, College of Health Sciences,
 Eulji University, Seongnam, Korea
[b]School of Life Sciences and
 Biotechnology, Korea University,
 Seoul, Korea
[c]Departments of Pathology, [e]Pediatrics,
 and [d]Epilepsy Research Institute,
 Yonsei University College of Medicine,
 Seoul, Korea

Background and Purpose The pathogenesis of mitochondrial disease (MD) involves the disruption of cellular energy metabolism, which results from defects in the mitochondrial respiratory chain complex (MRC). We investigated whether infants with MRC I defects showed ultrastructural changes in skeletal muscle.

Methods Twelve infants were enrolled in this study. They were initially evaluated for unexplained neurodegenerative symptoms, myopathies, or other progressive multiorgan involvement, and underwent muscle biopsies when MD was suspected. Muscle tissue samples were subjected to biochemical enzyme assays and observation by transmission electron microscopy. We compared and analyzed the ultrastructure of skeletal muscle tissues obtained from patients with and without MRC I defects.

Results Biochemical enzyme assays confirmed the presence of MRC I defects in 7 of the 12 patients. Larger mitochondria, lipid droplets, and fused structures between the outer mitochondrial membrane and lipid droplets were observed in the skeletal muscles of patients with MRC I defects.

Conclusions Mitochondrial functional defects in MRC I disrupt certain activities related to adenosine triphosphate synthesis that produce changes in the skeletal muscle. The ultrastructural changes observed in the infants in this study might serve as unique markers for the detection of MD.

Key Words mitochondria, respiratory chain complex, infant, muscle pathology, ultrastructure, transmission electron microscopy.

INTRODUCTION

Defects in the mitochondrial respiratory chain complex (MRC) can disrupt cellular energy metabolism, resulting in mitochondrial disease (MD), which is an inherited metabolic disorder.[1] MRC defects can influence cellular function in various ways, with the neuromuscular system typically being affected.[2] Diagnosing MD is a challenge because of its genetic heterogeneity, diversity in clinical phenotypes, and the lack of gold-standard diagnostic criteria.[3] The diagnosis involves evaluating clinical symptoms, performing imaging studies and biochemical enzyme assays, and assessing the pathology and molecular biology. MD in infants is particularly difficult to diagnose because the presentation usually involves clinical symptoms that are either atypical or similar to numerous other diseases.[4,5]

 Muscle biopsy is the most helpful diagnostic procedure for evaluating MD, especially when other tests produce normal findings.[6,7] While the presence of dramatic crystalline inclusions in the mitochondria of skeletal muscle is considered an ultrastructural change characteristic of biopsied skeletal muscle in adults with MD, wide variations in the changes in the ultrastructure of mitochondria in infants with MD have been reported, including between

organ types and MD classifications.

Since morphological changes in the mitochondria of infants with MD have not been characterized adequately, we investigated the associated ultrastructural changes in the skeletal muscle.

METHODS

Patients and muscle biopsy

Twelve infants were enrolled in this study. They were initially evaluated for unexplained neurodegenerative symptoms, myopathies, or other progressive multiorgan involvement. Each patient underwent a biopsy of the quadriceps muscle when MD was suspected. Lactic acidosis was defined as an increase of more than twice the normal reference value. The level of serum creatine kinase was normal in all patients.

Biochemical enzyme assays of muscle tissue confirmed the presence of MRC I defects in 7 of the 12 patients. Only subjects confirmed by the assay as MRC I were categorized as patients in order to ensure homogeneity of the disease state. Mitochondrial enzyme functions were evaluated by analyzing the activities of reduced nicotinamide adenine dinucleotide (NADH)-coenzyme Q (CoQ) reductase (complex I), succinate-CoQ reductase (complex II), succinate-cytochrome c reductase (complex II and III), cytochrome c reductase (complex III), cytochrome c oxidase (complex IV), oligomycin-sensitive ATPase (complex V), and citrate synthase. The activities of these complexes were assessed in isolated mitochondria obtained from muscle tissue using standard spectrophotometric assays, as described by Rustin et al.[8] We defined MRC defects as a reduction of the residual enzyme activity to below 10% of that in controls. The seven patients with MRC I defects also satisfied the definitive diagnostic criteria described by Bernier et al.[9] Five of the original 12 patients did not exhibit defects in biochemical enzyme assays and did not satisfy the criteria for MD, and so were categorized as the control group without MD.

Transmission electron microscopy was performed using samples from patients with MRC I defects and control patients without enzymatic defects. The study protocol was approved by the Institutional Review Board of Yonsei University Gangnam Severance Hospital, and written informed consent was obtained from the parents or legal guardians of all patients (IRB No. 3-2010-0190).

Sample preparation for electron microscopy

Samples were fixed in 2.5% glutaraldehyde mixed with 2% paraformaldehyde solution (0.1 M cacodylate buffer, pH 7.0) for 1 hour and then in 2% osmium tetroxide for 1 hour at 4°C. The samples were stained en bloc with 2% uranyl acetate, followed by dehydration with a graded acetone series and embedding in low-viscosity medium.

Conventional transmission electron microscopy and image analysis

Samples were sectioned at 60 nm using an ultramicrotome (MTXL, RMC, Tucson, AZ, USA). The sections were double-stained with 2% uranyl acetate for 20 minutes and lead citrate for 10 minutes, then viewed with the aid of transmission electron microscopy operating at 120 kV (Tecnai 12, FEI, Netherlands; H-7600, Hitachi, Tokyo, Japan).

The total number of intermyofibrillar mitochondria per 100 μm^2 was counted in each group. The concentration of intermyofibrillar mitochondria was also checked in each patient with and without MRC I defects. Every sample was photographed within a randomly selected grid square. The total counts of mitochondria were divided by the total measured area in order to calculate the number of mitochondria per square micron. Finally, the mitochondria density was expressed as the mean number of mitochondria per 100 μm^2. Statistical analysis was performed using Student's t-test.

The sizes of 50 randomly chosen mitochondria and lipid droplets were measured in each patient using the Image J program (National Institutes of Health). Mitochondria and lipid droplets were circled, and their actual size was calculated using a calibration grid. Values were represented as the mean individual size (in square microns) of mitochondria and lipid droplets. The statistical significance of differences between means was assessed by analysis of variance followed by Student's t-tests. A probability of less than 5% was considered significant ($p < 0.05$). Statistical normalization was used to investigate the relationship between mitochondria and lipid droplets.

Three-dimensional structure of lipid droplets and mitochondria

For the reconstruction of the three-dimensional (3D) structure, electron tomography (H-7600) was performed with 60-nm-thick sections collected on formvar/carbon-coated copper slot grids and stained with uranyl acetate and lead citrate. Colloidal gold particles were applied to both sides of sections as fiducial markers. A series of 61 tilted images was recorded around a tilt axis over an angular range of 120° with a tilt interval of 2°. Images were aligned and surface-rendered models were produced using IMOD (The Mastronarde Group, Boulder, CO, USA).[10,11]

RESULTS

Diagnosis of patients

Central nervous system involvement was observed in all pa-

tients, with this involving multiple organs in most cases. All of the patients showed background slowing in electroencephalograms, which is consistent with encephalopathy, and various degrees of involvement in brain magnetic resonance imaging (MRI). Patients in both groups (patients with MRC I defects and control patients without enzymatic defects) showed various clinical characteristics (Table 1 and 2). The findings for all enzyme assays other than for MRC I defects were normal. One of the patients with MRC I defects was diagnosed with Leigh syndrome as a clinical subtype of MD, while the other six patients had nonspecific encephalopathy. The patient with Leigh syndrome exhibited typical findings of lactic acidosis and basal ganglia involvement in brain MRI. Light-microscopy examination of the muscle tissues revealed no ragged-red fibers. Modified Gomori trichrome and other special immunohistochemical staining procedures yielded normal results.

MRC I defects, mitochondrial size, and structural changes in cristae

To determine whether MRC I defects caused ultrastructural changes, we compared the ultrastructure of skeletal muscle in the patients. Enzyme tests revealed that 7 of the 12 originally enrolled patients had MRC I defects (Table 1), while the remaining 5 patients were included as control individuals for comparison. Quantification of these changes showed differences in mitochondrial size and cristae area between muscles with and without MRC I defects (Fig. 1D and E), while there were no intergroup differences in mitochondrial numbers (Fig. 1F). The mean mitochondrial sizes were 0.21 ± 0.07 and 0.10 ± 0.03 μm^2 in patients with and without MRC I defects, respectively (Fig. 1D). Thus, the mitochondria in patients with MRC I defects were 53% larger than those in patients without such defects (p=0.005) (Fig. 1A-C). In patients with MD, the cristae area represented $17.4\pm3.0\%$ of the total mitochondrial area in mitochondria from patients without MRC I defects and $7.8\pm1.8\%$ in mitochondria from patients with these defects, representing a 2.2-fold difference (Fig. 1B, C, and E). Moreover, compared with the tubular structure of cristae in mitochondria from patients without MD (Fig. 1A), patients with MRC I defects exhibited elongated, curved cristae that were frequently stacked against one another (Fig. 1B). Other obvious structural changes included irregularly shaped mitochondria containing numerous internal vesicles (Fig. 1C).

MRC I defects and lipid droplets in muscle

A particularly interesting finding was that ultrastructure images of skeletal muscle showed that the number of intramyocellular lipid droplets (IMCLs) was greater in patients with MRC I defects (Fig. 2B and D) than in those without defects

Table 1. Patient characteristics

Patient no.	1	2	3	4	5	6	7	8	9	10	11	12
Sex	Female	Male	Male	Male	Female	Female	Female	Female	Female	Male	Male	Male
Initial symptom	Hypotonia	Seizure	Seizure	Failure to thrive	Hypotonia	Microcephaly	Failure to thrive	Seizure	Hepatomegaly	Hypotonia	Hypotonia	Strabismus
Age at onset of initial symptom (months)	10	1	8	1	7	24	1	14	8	15	12	36
Progressive global developmental deterioration	+	+	+	+	+	+	+	+	+	+	+	+
Age at muscle biopsy (years)	1.5	1	3.9	1.9	3.3	2.6	1	2.1	1.9	5.1	1.8	9
Types of defects	MRC I	MRC I	MRC I	MRC I	MRC I	MRC I	MRC I	Normal	Normal	Normal	Normal	Normal
Distribution of organs involved												
CNS	+	+	+	+	+	+	+	+	+	+	+	+
Skeletal muscle	+	+	+	+	+	+	+	+	+	+	+	-
Heart	-	-	-	-	-	-	-	-	-	-	-	+
GI	+	+	-	-	+	-	-	-	+	-	-	-
Liver	-	-	-	-	-	-	-	-	+	-	-	-
Kidney	+	-	-	-	+	-	-	-	+	-	-	-
Eyes	+	-	-	-	-	-	-	-	-	-	-	+
Hearing	-	-	-	-	-	-	-	-	+	-	-	-

CNS: central nervous system, GI: gastrointestinal tract, MRC: mitochondrial respiratory chain complex.

Table 2. Clinical subtype of MD and brain MRI findings

Patient no.	Clinical subtype of MD	Lactic acidosis*	Involved area in brain MRI							
			Basal ganglia	Thalamus	Brain stem	Cerebellum	Cortex	White matter	Diffuse atrophy	Infarction
1	Nonspecific encephalomyopathy	+	–	–	–	+	+	+	+	–
2	Nonspecific encephalomyopathy	+	–	–	–	+	+	+	+	–
3	Nonspecific encephalomyopathy	–	–	–	–	–	+	+	+	–
4	Leigh syndrome	+	+	+	–	–	–	+	–	–
5	Nonspecific encephalomyopathy	+	–	–	–	–	+	+	+	–
6	Nonspecific encephalomyopathy	+	–	–	–	–	+	+	–	–
7	Nonspecific encephalomyopathy	–	–	–	–	–	–	–	+	–

*More than twofold higher than the normal reference value.
MD: mitochondrial disease, MRI: magnetic resonance imaging.
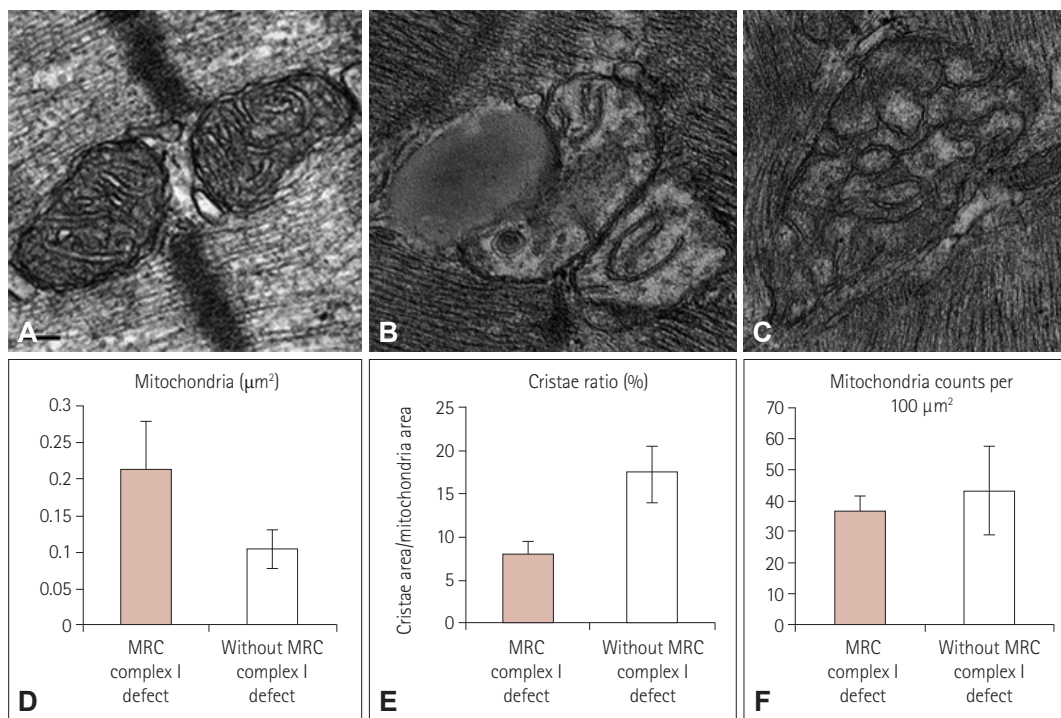

Fig. 1. Transmission electron microscopy of human mitochondria in skeletal muscle. Mitochondria in muscle without (A) and with (B and C) MRC I defects. Mitochondrial size is shown in (D). Changes in the percentage area of cristae and the mitochondrial size are shown in (E). The number of mitochondria is counted in (F). The number of mitochondria per square micron was multiplied by 100 to calculate the number of filaments per 100 μm^2. Scale bars indicate 100 nm. MRC: mitochondrial respiratory chain complex.

(Fig. 2A and C). Lipid droplets were frequently observed adjacent to the mitochondria in two-dimensional images (Figs. 1B and 2D). The size of IMCLs differed significantly (Fig. 2G), being 0.2127±0.0462 and 0.0647±0.0139 μm^2 in patients with and without MRC I defects, respectively, indicating a difference of more than threefold (Fig. 2G). Statistical normalization was applied to the data to study the relationship between structural changes of mitochondria and size increases in lipid droplets in patients. A positive correlation between lipid droplet size and mitochondrial size was observed consistently in all of the patients.

Lipid droplets were surrounded by one or multiple mitochondria (Fig. 2D). Electron tomography was applied to improve the resolution of the obtained images and thereby allow a more detailed structural analysis of lipid droplets and mitochondria. The electron tomograms showed that lipid droplets were in direct contact with mitochondria (Fig. 2E), and analysis of the 3D structure confirmed that the outer mitochondrial membrane was directly connected to the surrounding lipid droplets (Fig. 2F).
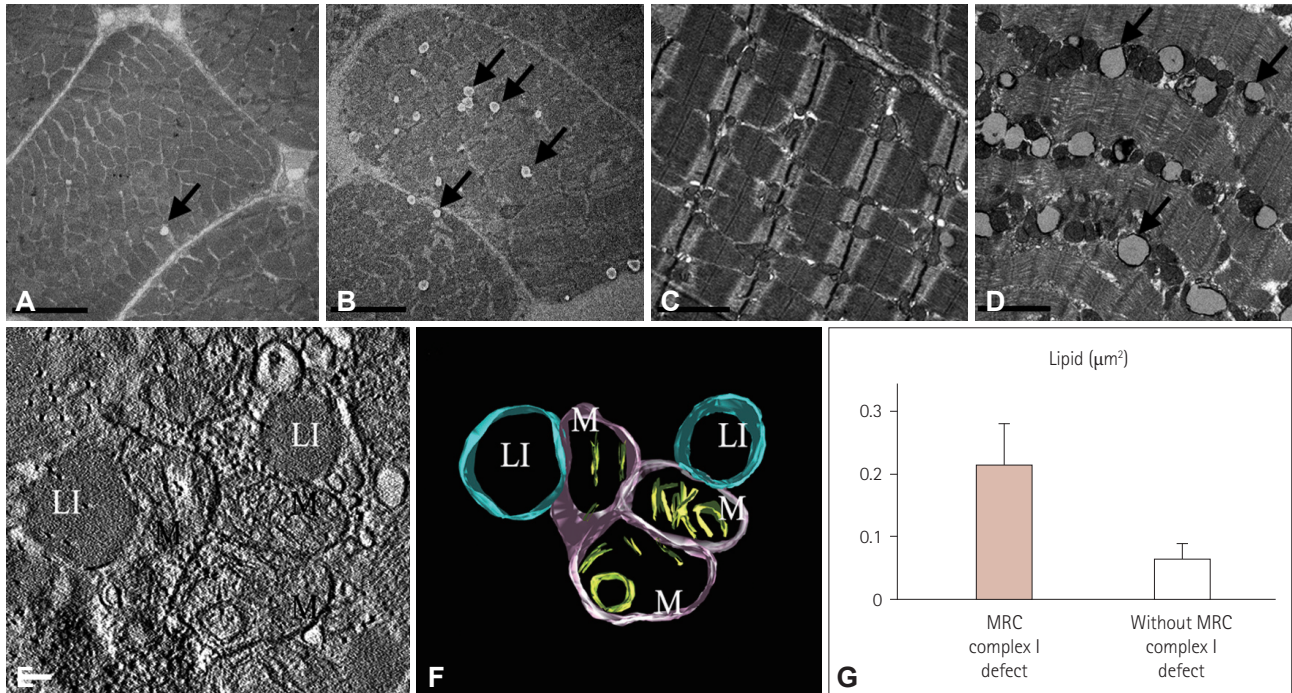
Fig. 2. Effects of mitochondrial dysfunction on intramyocellular lipid droplets. These are images from patients without (A and C) and with (B and D) MRC I defects. Arrows indicate lipid droplets. Electron tomograms are illustrated in (E). The 3D reconstruction of mitochondria and lipid droplets are shown in (F). The outer membrane of the mitochondria is shown in pink and cristae in green. Sizes of lipid droplets were presented as the mean values for 50 lipid droplets measured in each group (G). Scale bars indicate 5 μm (A and B), 2 μm (C and D), and 100 nm (E). Li: lipid droplet, M: mitochondria, MRC: mitochondrial respiratory chain complex.

DISCUSSION

Mitochondrial volume homeostasis is a housekeeping cellular function that helps to regulate oxidative capacity, apoptosis, and mechanical signaling. Changes in the mitochondrial volume have been shown to be associated with a wide range of important biological functions and pathologies. To our knowledge, the present study is the first to investigate the mitochondrial size and ultrastructural features of skeletal muscle of infants with MRC I defects. The mitochondrial volume is primarily regulated by the potassium flux into and out of the matrix, and is controlled by the electrochemical potential. However, the mitochondrial volume may be altered in the presence of various disorders; for example, there are some reports of enlarged or swollen mitochondria resulting from functional disorders.[12-14] An increase in the mitochondrial volume has been shown to be related to a reduction in the mitochondrial membrane potential.[15] Moreover, an increased mitochondrial volume is often observed after mitochondrial depolarization, mitochondrial calcium overload, or opening of the permeability transition pore.[16] Another possible cause of mitochondrial swelling is the release of cytochrome c and apoptosis-inducing factor.[17]

The present study found significant increases in mitochondrial size in infants with MRC I defects but no definitive changes in the numbers of mitochondria. This finding could be due to the significant decrease in cristae. Abundant cristae are found in mitochondria from tissues having a high energy demand, and so decreases in cristae could be suggestive of the presence of functional defects.[18,19] The MRC plays a very important role in energy production and is mainly localized in the inner membrane, particularly within cristae.[20,21] Consequently, defects in the MRC could result in structural changes in mitochondria, particularly in cristae that are related to the oxidative capacity. When there is a lack of ATP synthase e or g subunits[22-24] and mitofilin, which is a part of the supramolecular complex of ATP synthase,[11,18,25] mitochondria manifest as an onion-like structure with decreased cristae and no cristae junctions. Enlarged mitochondria have also been observed in associated with a reduced cristae area, showing a honeycomb structure.[26] The present study frequently observed stacked cristae with reduced cristae junctions (resembling an onion-like structure) and interconnected cristae (resembling a honeycomb, vesicle structure) in the mitochondria of patients with MRC I defects. These structural changes indicate the presence of functional defects and imply that MRC I defects may be directly linked to ATP synthase. Furthermore, defects in this complex may affect lipid metabolism in mitochondria. Such morphological changes in mitochondria have not been clearly reported as a tool for differentiating between pediat-

ric and adult MD; however, changes in cristae area and mitochondrial size found in the tissues of patients with MRC I defects are of clinical importance, particularly in pediatric patients, and could indicate that MRC I defects are distinct from other types of MRC defects.

The mitochondrial membrane structure is dynamic and depends on the ATP level, apoptosis, oxidative stress, and aging.[27-29] Because the membrane dynamics of mitochondria affect mitochondrial function, more detailed analyses of morphological changes in the mitochondria of patients with MD have been performed. We applied electron tomography in order to improve the imaging resolution,[30] which yielded detailed images of the mitochondrial structure and direct connections between the mitochondrial outer membrane and lipid droplets. Lipid droplets wrapped by mitochondria reflect the intimate functional relationship between these two structures,[31] and these results were confirmed by statistical analysis. Statistical normalization suggested the presence of a mutual relationship between the increases in mitochondrial size and the number of lipid droplets. ATP is mainly produced by mitochondria via the utilization of glucose; however, other substances such as glycogen and lipid droplets can also be used to produce ATP. When skeletal muscle depends on lipids as an energy source, lipid accumulation may result from the impaired mitochondrial oxidation of fatty acids.[32,33] In addition, defects in lipid metabolism in mitochondria can affect mitochondrial transport to impair energy production, which is observed in progressive myopathies.[32]

Skeletal muscle is highly reliant on oxidative phosphorylation. Oxidative metabolism is linked to changes in mitochondrial structure and function. Although various changes in mitochondria have been reported in infants with mitochondrial dysfunction, no definitive characteristics have been consistently observed. Among the five complexes, MRC I (NADH: ubiquinone oxidoreductase) is the largest and most important mitochondrial enzyme. MRC I oxidizes NADH from the tricarboxylic acid cycle, promotes fatty-acid oxidation and glycolysis, reduces ubiquinone during the remaining steps of the respiratory chain, and transports protons across the inner mitochondrial membrane to support ATP synthesis. Defects in MRC I are the main well-known causes of MD.[34] However, studies of rare diseases such as MD are restricted by the small number of affected patients. In the present prospective study, we examined fresh biopsies of skeletal muscles in infants with or without MRC I defects. Patients were diagnosed based on clinical symptoms, the findings of imaging studies and biochemical enzyme assays, and assessing the pathology and molecular biology. Diagnosing MD in infants is especially difficult due to atypical clinical presentations and similarities with other diseases.[4,5]

The present findings suggest that mitochondrial functional defects in MRC I can disrupt certain activities related to ATP synthesis, resulting in changes in skeletal muscle. Although the seven infants with MRC I defects in this prospective study might be representative of this unique population, the findings cannot be generalized owing to the rarity of the disease. Despite this limitation, this study has provided a valuable starting point for clinicians to diagnose MD precisely and understand the natural course of MRC I defects in the pediatric population. The ultrastructural changes in mitochondria and lipid droplets in infant patients with MRC I defects might be useful unique markers for detecting MD.

REFERENCES

1. McFarland R, Taylor RW, Turnbull DM. The neurology of mitochondrial DNA disease. *Lancet Neurol* 2002;1:343-351.
2. DiMauro S, Schon EA. Mitochondrial respiratory-chain diseases. *N Engl J Med* 2003;348:2656-2668.
3. Finsterer J. Mitochondriopathies. *Eur J Neurol* 2004;11:163-186.
4. Loeffen JL, Smeitink JA, Trijbels JM, Janssen AJ, Triepels RH, Sengers RC, et al. Isolated complex I deficiency in children: clinical, biochemical and genetic aspects. *Hum Mutat* 2000;15:123-134.
5. Miles L, Wong BL, Dinopoulos A, Morehart PJ, Hofmann IA, Bove KE. Investigation of children for mitochondriopathy confirms need for strict patient selection, improved morphological criteria, and better laboratory methods. *Hum Pathol* 2006;37:173-184.
6. McFarland R, Taylor RW, Turnbull DM. Mitochondrial disease--its impact, etiology, and pathology. *Curr Top Dev Biol* 2007;77:113-155.
7. Stadhouders AM, Jap PH, Winkler HP, Eppenberger HM, Wallimann T. Mitochondrial creatine kinase: a major constituent of pathological inclusions seen in mitochondrial myopathies. *Proc Natl Acad Sci U S A* 1994;91:5089-5093.
8. Rustin P, Chretien D, Bourgeron T, Gérard B, Rötig A, Saudubray JM, et al. Biochemical and molecular investigations in respiratory chain deficiencies. *Clin Chim Acta* 1994;228:35-51.
9. Bernier FP, Boneh A, Dennett X, Chow CW, Cleary MA, Thorburn DR. Diagnostic criteria for respiratory chain disorders in adults and children. *Neurology* 2002;59:1406-1411.
10. Duman JG, Pathak NJ, Ladinsky MS, McDonald KL, Forte JG. Three-dimensional reconstruction of cytoplasmic membrane networks in parietal cells. *J Cell Sci* 2002;115:1251-1258.
11. Mun JY, Lee TH, Kim JH, Yoo BH, Bahk YY, Koo HS, et al. Caenorhabditis elegans mitofilin homologs control the morphology of mitochondrial cristae and influence reproduction and physiology. *J Cell Physiol* 2010;224:748-756.
12. Chow CW, Thorburn DR. Morphological correlates of mitochondrial dysfunction in children. *Hum Reprod* 2000;15 Suppl 2:68-78.
13. Wang X, Li H, Zheng A, Yang L, Liu J, Chen C, et al. Mitochondrial

dysfunction-associated OPA1 cleavage contributes to muscle degeneration: preventative effect of hydroxytyrosol acetate. *Cell Death Dis* 2014 Nov [Epub]. https://doi.org/10.1038/cddis.2014.473.

14. Yang Y, Ouyang Y, Yang L, Beal MF, McQuibban A, Vogel H, et al. Pink1 regulates mitochondrial dynamics through interaction with the fission/fusion machinery. *Proc Natl Acad Sci U S A* 2008;105:7070-7075.

15. Safiulina D, Veksler V, Zharkovsky A, Kaasik A. Loss of mitochondrial membrane potential is associated with increase in mitochondrial volume: physiological role in neurones. *J Cell Physiol* 2006;206:347-353.

16. Kaasik A, Safiulina D, Zharkovsky A, Veksler V. Regulation of mitochondrial matrix volume. *Am J Physiol Cell Physiol* 2007;292:C157-C163.

17. Petit PX, Goubern M, Diolez P, Susin SA, Zamzami N, Kroemer G. Disruption of the outer mitochondrial membrane as a result of large amplitude swelling: the impact of irreversible permeability transition. *FEBS Lett* 1998;426:111-116.

18. John GB, Shang Y, Li L, Renken C, Mannella CA, Selker JM, et al. The mitochondrial inner membrane protein mitofilin controls cristae morphology. *Mol Biol Cell* 2005;16:1543-1554.

19. Zick M, Rabl R, Reichert AS. Cristae formation-linking ultrastructure and function of mitochondria. *Biochim Biophys Acta* 2009;1793:5-19.

20. Cogliati S, Frezza C, Soriano ME, Varanita T, Quintana-Cabrera R, Corrado M, et al. Mitochondrial cristae shape determines respiratory chain supercomplexes assembly and respiratory efficiency. *Cell* 2013;155:160-171.

21. Vogel F, Bornhövd C, Neupert W, Reichert AS. Dynamic subcompartmentalization of the mitochondrial inner membrane. *J Cell Biol* 2006;175:237-247.

22. Arselin G, Vaillier J, Salin B, Schaeffer J, Giraud MF, Dautant A, et al. The modulation in subunits e and g amounts of yeast ATP synthase modifies mitochondrial cristae morphology. *J Biol Chem* 2004;279:40392-40399.

23. Bustos DM, Velours J. The modification of the conserved GXXXG motif of the membrane-spanning segment of subunit g destabilizes the supramolecular species of yeast ATP synthase. *J Biol Chem* 2005;280:29004-29010.

24. Paumard P, Vaillier J, Coulary B, Schaeffer J, Soubannier V, Mueller DM, et al. The ATP synthase is involved in generating mitochondrial cristae morphology. *EMBO J* 2002;21:221-230.

25. von der Malsburg K, Müller JM, Bohnert M, Oeljeklaus S, Kwiatkowska P, Becker T, et al. Dual role of mitofilin in mitochondrial membrane organization and protein biogenesis. *Dev Cell* 2011;21:694-707.

26. Acehan D, Xu Y, Stokes DL, Schlame M. Comparison of lymphoblast mitochondria from normal subjects and patients with Barth syndrome using electron microscopic tomography. *Lab Invest* 2007;87:40-48.

27. Mannella CA. Structure and dynamics of the mitochondrial inner membrane cristae. *Biochim Biophys Acta* 2006;1763:542-548.

28. Scorrano L, Ashiya M, Buttle K, Weiler S, Oakes SA, Mannella CA, et al. A distinct pathway remodels mitochondrial cristae and mobilizes cytochrome c during apoptosis. *Dev Cell* 2002;2:55-67.

29. Ding WX, Li M, Biazik JM, Morgan DG, Guo F, Ni HM, et al. Electron microscopic analysis of a spherical mitochondrial structure. *J Biol Chem* 2012;287:42373-42378.

30. Mannella CA. Structural diversity of mitochondria: functional implications. *Ann N Y Acad Sci* 2008;1147:171-179.

31. Vock R, Hoppeler H, Claassen H, Wu DX, Billeter R, Weber JM, et al. Design of the oxygen and substrate pathways. VI. structural basis of intracellular substrate supply to mitochondria in muscle cells. *J Exp Biol* 1996;199:1689-1697.

32. Bruno C, Bertini E, Di Rocco M, Cassandrini D, Ruffa G, De Toni T, et al. Clinical and genetic characterization of Chanarin-Dorfman syndrome. *Biochem Biophys Res Commun* 2008;369:1125-1128.

33. Harriman DG, Reed R. The incidence of lipid droplets in human skeletal muscle in neuromuscular disorders: a histochemical, electron-microscopic and freeze-etch study. *J Pathol* 1972;106:1-24.

34. Leonard JV, Schapira AH. Mitochondrial respiratory chain disorders I: mitochondrial DNA defects. *Lancet* 2000;355:299-304.